Progress In Electromagnetics Research, Vol. 156, 37–46, 2016

Meta-Loaded Circular Sector Patch Antenna

Sen Yan* and Guy A. E. Vandenbosch

Abstract—A circular sector patch antenna loaded with a periodic metamaterial topology is presented. Several shapes of the circular sector patch are analyzed, and the input impedances and radiation patterns are compared. The topology reveals a nearly constant resonant frequency at zeroth-order resonance (ZOR) while the radiation performance approaches the one of the ZOR full circular patch antenna. Compared with rectangular and circular patch antennas, the sector patch offers more tuning possibilities. A matching network can be easily introduced to enhance the impedance bandwidth. Apart from the ZOR characteristics, this topology can also support a quasi-monopolar pattern at multiple modes. A semicircular patch operating at 4.1 GHz together with an impedance matching network and a dual-band semicircular patch antenna are fabricated and measured.

1. INTRODUCTION

Flexible and compact antennas are becoming more important in portable devices such as mobile phones, laptops, GPSs, etc. The size of the antenna needs to be miniaturized while keeping the shape of the antenna flexible in order to suit different needs of the system. A lot of work has been done to realize Electrically Small Antennas (ESA), like the planar inverted-F antenna (PIFA), the meander transmission line antenna, and the loaded microstrip antenna [1–5].

In the recent decade, the application of metamaterials in antennas has invoked increasing interest. A metamaterial is a kind of artificial periodic structure with unique properties, which are not or hardly found in nature [6, 7]. As a kind of planar metamaterial, composite right/left handed transmission lines (CRLH-TL) [8] are widely used in antenna and circuit design, since it is easy to fabricate them on standard printed circuit board (PCB) [9]. A hotspot research field is the operation of the antenna at zeroth-order resonance (ZOR), where the wavelength is infinite, so that its operating frequency is independent of its physical size [8, 9]. The ZOR antenna can be designed much smaller than half a wavelength, enabling a very compact size [10, 11], or much larger than half a wavelength, in order to reach high directivity [12]. The CRLH-TL can also be used to design dual-band/multi-band antennas [13], circularly polarized antennas [18], and reconfigurable antennas [19], using their different resonant modes. Recently, the concept of CRLH TL has been introduced for coplanar waveguides (CPW) [20–22], and substrate integrated waveguides (SIW) [23, 24], which results in features like wide bandwidth and high efficiency.

While most of the antennas presented in literature are based on the linear CRLH-TL with mushroom structure, a radial topology is also possible. In [25] a circuit model for the radial CRLH-TL structure is introduced and a circular patch antenna loaded with a CRLH-TL is analyzed. The size of the antenna is further miniaturized in [26]. A significant advantage of the circular patch is that it can provide an extremely symmetric radiation pattern. In this paper, the circular sector patch antenna loaded with a metamaterial is discussed. It will be shown that for this type of sector antenna the resonant frequency of the ZOR mode is almost the same as in the case where the whole circle is used. First of all, this

Received 9 February 2016, Accepted 2 May 2016, Scheduled 5 May 2016
* Corresponding author: Sen Yan (sen.yan@esat.kuleuven.be).
The authors are with the ESAT-TELEMIC, KU Leuven, Kasteelpark Arenberg 10, Leuven, B-3001, Belgium.

can help to further reduce the size of antenna. Second, the space that becomes available can be used to introduce an impedance matching network in order to provide a wider bandwidth compared to the full circular patch antenna. The proposed radial patch structure can also serve as a basis for dual-band or multi-band antennas featuring different modes. Since the feeding point is located at the center, the whole working band shows a quasi-omnidirectional radiation pattern. The frequency ratio can be freely selected by tuning the interdigital capacitors.

In Section 2, the basic structure, i.e., the complete circular patch antenna, is briefly overviewed. In Section 3, several circular sector patch antennas are numerically compared for their resonant frequencies, input impedances, radiation efficiencies, and directivities. Section 4 discusses a feeding circuit for impedance matching of a semicircular patch and one design is fabricated and measured. The dual-band antenna is discussed in Section 5.

2. CIRCULAR PATCH ANTENNA

A typical mushroom CRLH-TL circular patch antenna topology is shown in Fig. 1(a). The slots between the rings provide the series capacitances and the metallic pins supply the shunt inductances for the transmission line. The series inductances and shunt capacitances are induced by the equivalent distribution parameters of the transmission line itself [8]. In order to obtain a quasi-homogeneous medium, all the unit cells (rings) have the same width. The pins are positioned in the geometric center of each ring, and the number of pins in each unit cell is directly proportional to the size of the ring [25]. The CRLH-TL can be recognized as a double negative metamaterial, which can form negative modes. An alternative, the inductor loaded structure, is displayed in Fig. 1(b). This structure only differs from the CRLH-TL (Fig. 1(a)), by the fact that the slots between the unit cells are absent. This inductor loaded structure is in essence a kind of epsilon negative metamaterial. It has similar radiation characteristics at the ZOR mode and the positive modes. However, it cannot support the negative modes. Both the CRLH-TL and inductor loaded structure can be analyzed based on the concept of a radial transmission line topology. A circuit model already has been proposed in [25].

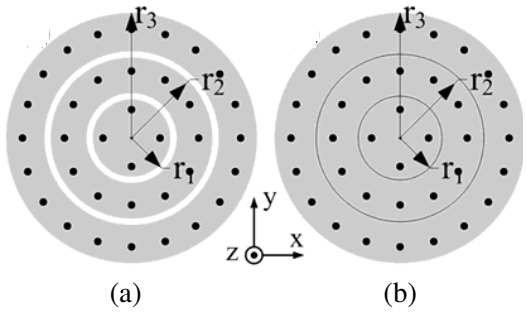

Figure 1. Topology of circular patch antenna with meta-loading. (a) CRLH-TL loaded structure, (b) Inductor loaded structure.

3. CIRCULAR SECTOR PATCH ANTENNA

For a circular patch antenna operating in ZOR mode, the electric field under the patch is nearly constant in both the azimuthal and the radial direction. It is reasonable to assume that just a sector of the circular patch can also support the same ZOR mode as the circular patch.

In the following, we will analyze the circular sector patch antennas shown in Fig. 2. The substrate used is Rogers RO 4003 ($\varepsilon_r = 3.55$, $\tan\delta = 0.0027$) with thickness 1.524 mm, and the width of each unit cell is 10 mm ($r_1 = r_2/2 = r_3/3$). The width of the gap between the copper rings is 0.3 mm, and the number of the pins in the unit cells is given in Fig. 2. The diameter of the pins is 0.5 mm. The antennas are fed by a probe in the center of the circle. In all structures, the size of the substrate and the ground is $120 \times 120\,\text{mm}^2$, and the center points of all the sectors are located in the center of the

substrate. The minimum distance from the patch to the edge of the substrate is 30 mm, which is larger than a half wavelength at the operating frequency.

CST microwave studio was used to perform a numerical analysis of all sector patch antennas in Fig. 2, working in the ZOR mode. Table 1 compares the resonant frequencies, input impedances, radiation efficiencies, and directivities.

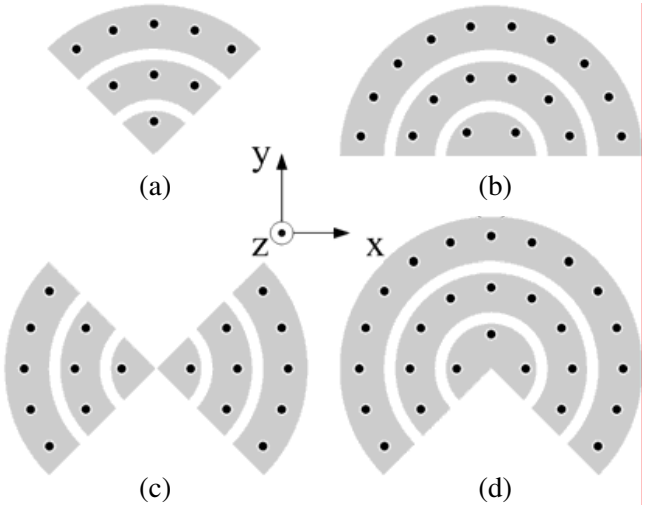

Figure 2. Several circular sector patch antenna types. (a) a quarter sector (90°), (b) semicircular sector (180°), (c) double quarter sector (each sector is 90°), (d) three quarter sector (270°).

Table 1. Changing the width of the unit cell.

	Shape	f_0 (GHz)	$Z_{in} = R_{in} + jX_{in}$ (Ω)	Rad. eff. (dB)	Dir. (dB)
CRLH-TL	Fig. 2(a)	4.135	104.4+j51.3	−0.51	7.1
	Fig. 2(b)	4.262	74.1+j82.4	−0.44	7.2
	Fig. 2(c)	4.115	98.2+j79.8	−0.84	7.1
	Fig. 2(d)	4.34	66.4+j93.1	−0.54	6.6
	Fig. 1(a)	4.495	46.8+j102.3	−0.44	5.4
Inductor loaded structures*	Fig. 2(a)	4.085	268.7+j160.9	−0.50	6.67
	Fig. 2(b)	4.232	89.2+j122.6	−0.44	7.03
	Fig. 2(c)	4.13	170.2+j119.2	−0.84	7.2
	Fig. 2(d)	4.3	56.2+j115.1	−0.55	6.6
	Fig. 1(b)	4.435	22.9+j115.2	−0.52	5.6

*The shapes of the circular sector patches loaded with the inductor loaded structures are almost the same as in Fig. 2, but without slots, as depicted in Fig. 1(b).

First of all, it is important to note that, although there is a large variation in antenna size, all resonant frequencies are nearly the same. The maximum difference is about 10%, both for the CRLH and inductor loaded antennas. This characteristic of the ZOR antenna gives engineers quite some freedom to choose the shape of the antenna in a dedicated way for a specific compact system. The efficiency of the antennas remains at a high level even with decreasing size. The directivities are higher than the one for the full circle. This is due to the fact that the radiation patterns become asymmetric, which is caused by the loss of the circular symmetry of the patch itself. The highest directivities are

found for the b and c structures. The only parameter changing considerably is the input impedance. The input impedance is continuously increasing as the size is decreasing. This means that special feeding methods, including an impedance matching, are needed.

It was also clearly observed that the effect of other physical parameters (e.g., the number of unit cells, the width of the unit cells, the number of pins, etc.) on the antenna characteristics is similar as in case of the whole circular patch antenna, see [25].

4. SEMICIRCULAR PATCH WITH MATCHING NETWORK

All the topologies in Fig. 2 can be used as the radiator. However, in real applications the symmetry of the radiation pattern has to be considered. In this section the design flow for the matching network of a semicircular patch is given. The same concept can be used for the other topologies of Fig. 2. Table 1 shows that the input impedance is far from 50 Ω, which means that an impedance matching network is indeed necessary in order to feed power efficiently. In [25], coaxial cable feeding from the back of the antenna is used, with a slot near the feeding point for impedance matching. In this paper a microstrip feeding line is used. It can provide more bandwidth than the coaxial feeding.

Figure 3(a) shows the details of the feeding network used. An interdigital capacitor and an additional transmission line provide the matching. For different circular sectors, different values for the capacitor have to be used. This can be reached by changing the number, width, spacing and length of the fingers, and the width and length of the transmission line. The genetic algorithm integrated in CST is used to optimize this matching network in order to obtain the smallest possible return loss. A semicircular sector patch is used to illustrate the topology. The optimium dimensions are discribed in Fig. 3(a) and Table 2. A prototype was fabricated and is shown in Fig. 3(b).

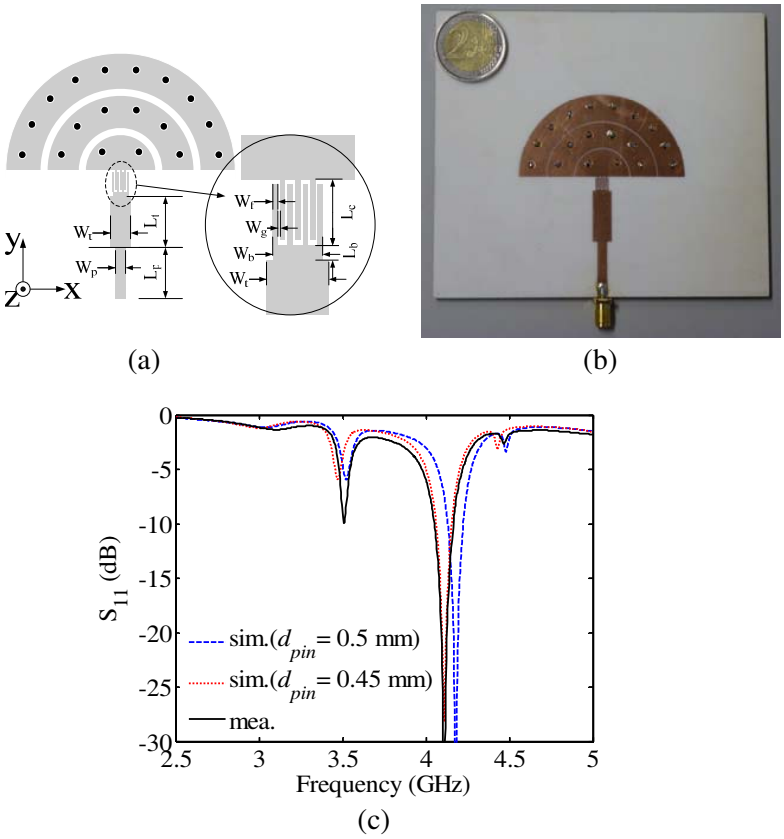

Figure 3. Semicircular sector patch antenna with matching network. (a) Topology. (b) Fabricated prototype. (c) Reflection coefficient.

The reflection coefficient of the prototype is measured with an Agilent Vector Network Analyzer 8510. The simulated and measured results are displayed in Fig. 3(c). The order of a mode can be uniquely determined based on the field distribution. A significant ZOR resonance can be observed. However, the measured result (4.109 GHz) shows a noticeable shift to lower frequencies compared to the original simulations. The reason is that the metallic wires used as vias are narrower than the diameters of the holes in the PCB, and that the soldering tin cannot fill the gaps between wires and holes completely. Using the real diameter of the wires in the simulation, i.e., 0.45 mm, the result agrees much better, as shown in Fig. 3(c). Meanwhile, a small resonance can also be observed around 3.462 GHz, which corresponds to the $n = -1$ mode. The $n = -2$ mode can hardly be seen due to mismatching.

Table 2. The parameters of the feeding network (Unit: mm).

W_p	L_p	W_t	L_t	W_f	W_g	L_c	W_b	L_b
3.45	20	6.8	18	0.4	0.3	4.5	4.6	0.5

Table 3. Simulated and measured results.

	Freq. (GHz)	S_{11} (dB)	BW (MHz)	Dir. (dBi)	Gain (dBi)	Eff. (%)
Simulated	4.110	−28	91	6.34	5.65	85
Measured	4.109	−57	114	/	5.82	82

The simulated z component of the electric field (E_z) is shown for the $n = -1$ and the ZOR mode in Fig. 4. For the $n = -1$ mode (3.462 GHz), E_z has a standing wave behavior in the radial direction from the center of the patch to the edge. For the $n = 0$ mode (4.110 GHz), the field distribution is totally different. The electric field is nearly constant under the patch, in both azimuthal and radial direction, which is characteristic for the ZOR mode.

The far field of the antenna was measured in the anechoic chamber of KU Leuven. The radiation pattern of the ZOR mode is shown in Fig. 5. The measured results agree well with the simulated ones. The only difference is the back radiation, which is caused by the presence of the feeding coaxial cable in the measurement set-up. The semicircular sector patch shows a vertical polarization and a quasi-monopolar pattern in the x-y plane. The omnidirectionality is not as good as for the circular patch. On the z-axis, the θ component of the electric field is zero, as in the case of a monopole. The maximum radiation level is observed at about $\theta = 40°$ and $\varphi = 90°$. Several other important parameters of the antenna are given in Table 3. The cross polarization in the y-z plane is mainly due to the feeding lines.

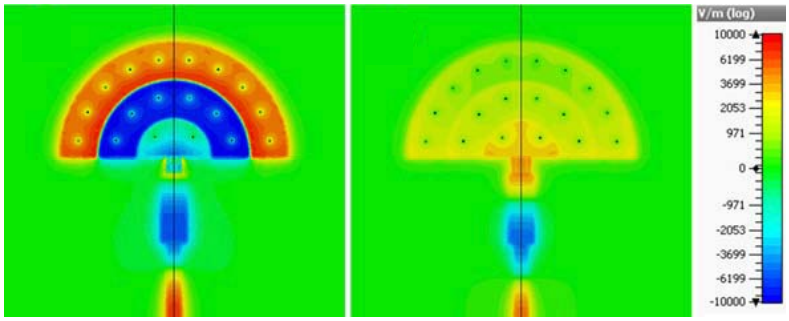

(a) (b)

Figure 4. Distribution of z component of the electric field. (a) 3.462 GHz, (b) 4.110 GHz.

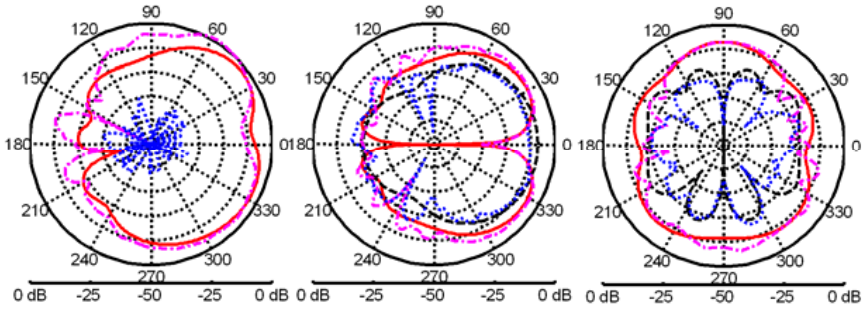

Figure 5. Radiation patterns of the semicircular patch antenna at 4.11 GHz. (a) y-z plane ($\theta = 90°$), (b) x-z plane ($\varphi = 0°$), (c) x-y plane ($\varphi = 90°$). The coordinate system is defined as in Fig. 3(a). (solid (red) line: simulated θ component, dashdot (magenta) line: measured θ component, dashed (black) line: simulated φ component, dotted (blue) line: measured φ component.)

5. DUAL-BAND SEMICIRCULAR PATCH ANTENNA

It has been shown in Fig. 3 that the CRLH-TL antenna can support a dual-band behavior. However, two issues need to be studied: one is the tuning of the frequency ratio; the other is the impedance matching. Here, interdigital capacitors are introduced to replace the series slot capacitors, see Fig. 6(a). By changing the number, length and width of the fingers, the left-handed capacitor (C_L) can be easily adjusted to control the tuning of the frequency ratio. Fig. 6(b) shows the resonant frequency for different lengths of the capacitor fingers. The radius of the whole patch (R) is fixed at 40 mm. As the ratio of Sl and r_1 is increasing, the resonant frequency of the ZOR mode only slightly decreases, since it is not related to the left-handed capacitors (C_L), as explained in [25]. However, the resonant frequencies of the other two (negative) modes are decreasing, as C_L becomes larger. By tuning the shape of the patch (sl/r_1), the frequency ratio of the modes can be easily adjusted.

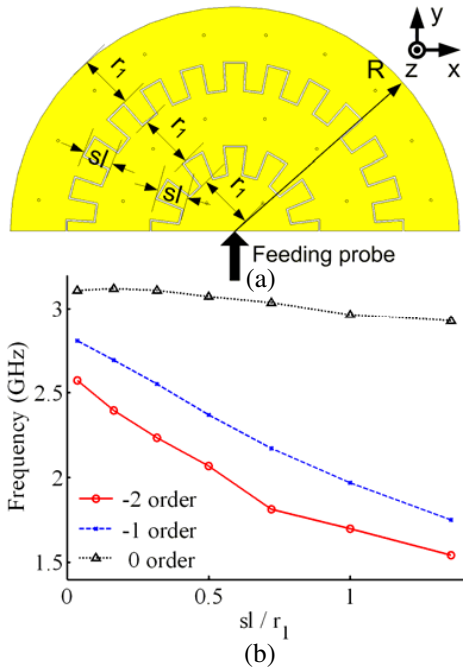

Figure 6. (a) Model of the multi-band semicircular patch, (b) the resonant frequencies of the patch.

After obtaining the required frequency ratio, the double stub tuning method can be used to form a matching network. An example is displayed in Figs. 7(a) and 7(b), in which r_1 and sl is 10 mm and 5 mm, respectively. The dimensions of the double stub matching network are optimized to obtain the minimum return loss at the $n = -1$ mode and the ZOR mode. The measured results are in Fig. 7(c). A high qualitative agreement is observed. The slight frequency shifts are easily explained by the tolerances on the material parameters and the fabrication dimensions.

The pattern of the antenna is measured in an anechoic chamber and is shown in Fig. 8. Note that the antenna displays a monopolar pattern at each resonant frequency. This is very attractive in many communication systems. The performance of the antenna is given in Table 4. Since the efficiency at

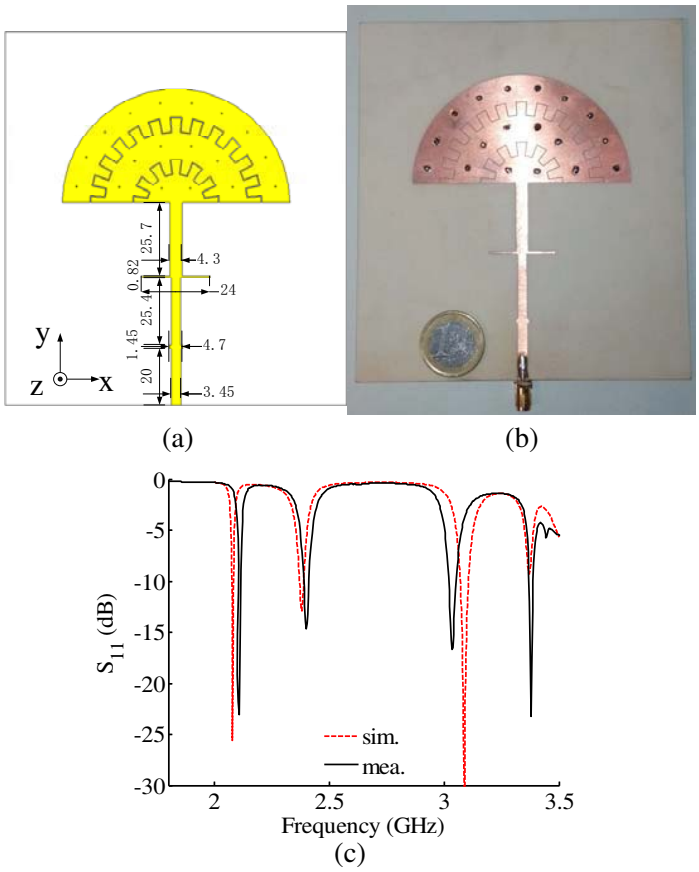

Figure 7. Dual-band semicircular patch antenna with matching network. (a) Topology, (b) fabricated prototype, (c) measured and simulated S_{11}.

Table 4. Simulated and measured results.

		Freq. (GHz)	S_{11} (dB)	BW (MHz)	Dir. (dBi)	Gain (dBi)	Eff. (%)
$n = -2$	Sim.	2.080	−25.6	8	6.1	−1.5	22
	Mea.	2.105	−23.0	10	/	−1.8	27
$n = -1$	Sim.	2.380	−12.9	17	6.5	4.9	67
	Mea.	2.394	−14.7	21	/	5.1	64
$n = 0$	Sim.	3.088	−43.5	35	6.6	5.2	74
	Mea.	3.033	−16.7	32	/	5.8	75

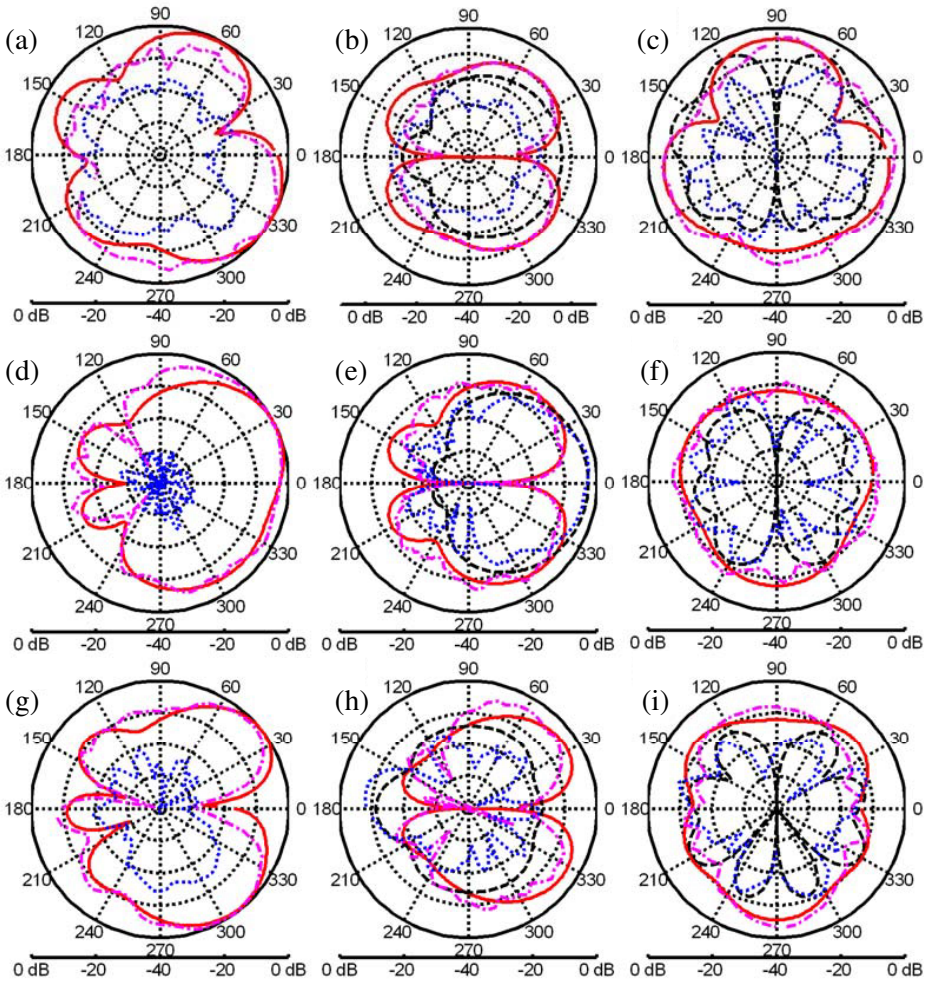

Figure 8. Radiation patterns of the semicircular patch antenna. (a) y-z, (b) x-z, (c) x-y plane at 2.08 GHz, (d) y-z, (e) x-z, (f) x-y plane at 2.38 GHz, (g) y-z, (h) x-z, (i) x-y plane at 3.03 GHz. The coordinate system is defined as in Fig. 7(a). (solid (red) line: simulated θ component, dashdot (magenta) line: measured θ component, dashed (black) line: simulated φ component, dotted (blue) line: measured φ component.)

$n = -2$ mode is very low, the antenna is proposed to operate at $n = -1$ mode and ZOR mode. The $n = +1$ mode is also matched at 3.37 GHz. It is possible to tune this mode to a desired frequency, but this is not considered in this design.

6. CONCLUSION

In this paper, the meta-loaded circular sector patch antenna topology is introduced. Several sector shapes are analyzed concerning resonant frequencies, input impedances, radiation efficiencies, and directivities. Since the operating frequency is chosen at the ZOR mode, all sector antennas considered have similar resonant frequencies and a similar radiation pattern. A semicircular sector patch antenna with microstrip impedance matching network is fabricated and measured. The simulated and measured results coincide very well and show that the antenna radiates efficiently as a monopole. A dual-band semicircular patch antenna is also designed and shows a quasi-monopolar pattern at both working frequencies.

REFERENCES

1. Garg, R., P. Bhartia, I. Bahl, and A. Ittipiboon, *Microstrip Antenna Design Handbook*, Artech House, 2001.
2. Wong, K. L., *Compact and Broadband Microstrip Antennas*, Wiley, 2002.
3. Kumar, G. and K. P. Ray, *Broadband Microstrip Antennas*, Artech House, 2003.
4. Soh, P. J., G. A. E. Vandenbosch, S. L. Ooi, and H. M. R. Nurul, "Design of a broadband all-textile slotted PIFA," *IEEE Transactions on Antennas and Propagation*, Vol. 60, No. 1, 379–384, Jan 2012.
5. Soh, P. J., S. J. Boyes, G. A. E. Vandenbosch, Y. Huang, and S. L. Ooi, "On-body characterization of dual-band all-textile PIFAs," *Progress In Electromagnetic Research*, Vol. 129, 517–539, 2012.
6. Shelby, R. A., D. R. Smith, and S. Schultz, "Experimental verification of a negative index of refraction," *Science*, Vol. 292, 77–79, 2001.
7. Yan, S. and G. A. E. Vandenbosch, "Increasing the NRI bandwidth of dielectric sphere-based metamaterials by coating," *Progress In Electromagnetics Research*, Vol. 132, 1–23, 2012.
8. Lai, A., C. Caloz, and T. Itoh, "Composite right/left-handed transmission line metamaterials," *IEEE Microwave Magazine*, Vol. 5, 34–50, Sept .2004.
9. Caloz, C., T. Itoh, and A. Rennings, "CRLH metamaterial leaky-wave and resonant antennas," *IEEE Antennas and Propagation Magazine*, Vol. 50, 25–39, Oct. 2008.
10. Lee, C.-J., K. M. K. H. Leong, and T. Itoh, "Composite right/left-handed transmission line based compact resonant antennas for RF module integration," *IEEE Transactions on Antennas and Propagation*, Vol. 54, 2283–2291, Aug. 2006.
11. Lai, A., K. M. K. H. Leong, T. Itoh, "Infinite wavelength resonant antennas with monopolar radiation pattern based on periodic structures," *IEEE Transactions on Antennas and Propagation*, Vol. 55, 868–876, Mar. 2007.
12. Rennings, A., T. Liebig, S. Otto, C. Caloz, and I. Wolff, "Highly directive resonator antennas based on composite right/left-handed (CRLH) transmission lines," *2nd International ITG Conference on Antennas, 2007. INICA '07*, 190–194, Mar. 2007.
13. Herraiz-Martinez, F. J., V. Gonzalez-Posadas, L. E. Garcia-Munoz, and D. Segovia-Vargas, "Multifrequency and dual-mode patch antennas partially filled with left-handed structures," *IEEE Transactions on Antennas and Propagation*, Vol. 56, 2527–2539, Aug. 2008.
14. Yan, S., P. J. Soh, and G. A. E. Vandenbosch, "Compact all-textile dual-band antenna loaded with metamaterial inspired structure," *IEEE Antennas and Wireless Propagation Letters*, Vol. 14, 1486–1489, 2015.
15. Xu, H.-X., G.-M. Wang, and M.-Q. Qi, "A miniaturized triple-band metamaterial antenna with radiation pattern selectivity and polarization diversity," *Progress In Electromagnetics Research*, Vol. 137, 275–292, 2013.
16. Segovia-Vargas, D., F. J. Herraiz-Martínez, E. UgarteMuñoz, L. E. Garcá-Muñoz, and V. González-Posadas, "Quad-frequency linearly-polarized and dual-frequency circularly-polarized microstrip patch antennas with CRLH loading," *Progress In Electromagnetics Research*, Vol. 133, 91–115, 2013.
17. Yu, A., F. Yang, and A. Elsherbeni, "A dual band circularly polarized ring antenna based on composite right and left handed metamaterials," *Progress In Electromagnetics Research*, Vol. 78, 73–81, 2008.
18. Dong, Y., H. Toyao, and T. Itoh, "Compact circularly-polarized patch antenna loaded with metamaterial structures," *IEEE Transactions on Antennas and Propagation*, Vol. 59, 4329–4333, Nov. 2011.
19. Yan, S. and G. A. E. Vandenbosch, "Radiation pattern reconfigurable wearable antenna based on metamaterial structure," *IEEE Antennas and Wireless Propagation Letters*, DOI: 10.1109/LAWP.2016.2528299.

20. Jang, T., J. Choi, and S. Lim, "Compact coplanar waveguide (CPW)-fed zeroth-order resonant antennas with extended bandwidth and high efficiency on vialess single layer," *IEEE Transactions on Antennas and Propagation*, Vol. 59, No. 2, 363–372, Feb. 2011.
21. Wang, G. and Q. Feng, "A novel coplanar waveguide feed Zeroth-Order resonant antenna with resonant ring," *IEEE Antenna and Wireless Propagation Letters*, Vol. 13, 774–777, 2014.
22. Lee, H., D. J. Woo, and S. Nam, "Compact and bandwidth-enhanced asymmetric coplanar waveguide (ACPW) antenna using CRLH-TL and modified ground plane," *IEEE Antenna and Wireless Propagation Letters*, Vol. 15, 810–813, 2016.
23. Dong, Y. and T. Itoh, "Promising future of metamaterials," *IEEE Microwave Magazine*, Vol. 13, No. 2, 39–56, Mar. 2012.
24. Yan, S., P. J. Soh, and G. A. E. Vandenbosch, "Wearable dual-band composite right/left-handed (CRLH) waveguide textile antenna for WLAN applications," *IET Electronics Letters*, Vol. 50, No. 6, 424–426, Mar. 2014.
25. Yan, S. and G. A. E. Vandenbosch, "Zeroth-order resonant circular patch antenna based on periodic structures," *IET Microwaves, Antennas & Propagation*, Vol. 8, No. 15, 1432–1439, Dec. 2014.
26. Yan, S., X. Wang, Y. Hu, and G. A. E. Vandenbosch, "Low profile omnidirectional antenna for automatic dependent surveillance — broadcast (ADS-B) applications," *IET Electronics Letters*, Vol. 51, No. 22, 1732–1734, Oct. 2015.